Rev.Adv.Mater.Sci. 14(2007) 174-182

BRITTLE FRACTURE OF 100-, 110-, 111-ORIENTED Cu CRYSTALS: MD *vs.* TB/MD APPROACH

Jacek Dziedzic[1], Michał Białoskórski[1,2] and Jarosław Rybicki[1,2]

[1]Faculty of Technical Physics and Applied Mathematics, Gdansk University of Technology, Narutowicza 11/12, 80-952 Gdansk, Poland
[2]TASK Computer Centre, Gdansk University of Technology, Narutowicza 11/12, 80-952 Gdansk, Poland

Received: February 20,2007

Abstract. Cross-scaling simulations of nanoindentation of copper with an infinitely hard tool, employing molecular dynamics concurrently augmented with tight-binding calculations, have been conducted for three crystal orientations of the workmaterial. The effect of introducing tight-binding into the calculation on the normal force experienced by the indenter and the displacement of workpiece atoms has been studied by comparing the results with pure molecular dynamics simulations.

1. INTRODUCTION

Ultra-precision machining, nanoscratching and nanoindentation belong to a class of technologically significant processes that have attracted considerable attention during the last two decades. Because of the submicron length scales involved, they are difficult and costly to study experimentally, which in turn entices researchers to attempt simulating them numerically.

Traditionally, such simulations employ the molecular dynamics (MD) method, wherein a system of classical particles interacting via an empirical potential is traced in discrete timesteps in the order of one femtosecond. Forces acting on every particle are obtained by analytical differentiation of the potential, while numerical integration of the equations of motion yields the positions and velocities of particles in subsequent timesteps. Nowadays, it is feasible to simulate systems containing hundreds of thousands of particles for time-scales in the order of a few nanoseconds using a typical workstation.

Although the molecular dynamics method has been used with success in this domain [1–6], its accuracy in the immediate region of contact between the tool and the workpiece is disputable. The reasons for this are twofold. Firstly, the potential with which the particles interact is parametrized so as to reproduce the properties of bulk material, where atoms are only slightly perturbed from their equilibrium positions. As soon as atoms become significantly displaced, as in the vicinity of the contact region, the forces obtained from the empirical potential become questionable. Secondly, as the molecular dynamics method neglects the presence of electrons altogether, no empirical potential can explicitly capture the details of bond-breaking and reconstruction taking place between the tool tip and the workmaterial.

Corresponding author: Jaroslaw Rybicki, e-mail: ryba@pg.gda.pl

Methods based on quantum dynamics can be used to account for the presence of electrons. However, with these the computational requirements become prohibitive for systems larger than a few hundred atoms. The least demanding approach that still manages to qualitatively capture electronic effects is the tight-binding (TB) method, which allows treatment of systems comprising of about 500 atoms in reasonable time.

Since the numbers of atoms in the systems in question are in the order of tens or hundreds of thousands, it is not feasible to treat all of them with the tight-binding formalism. Instead, simulations may be performed in a cross-scaling fashion, that is only the atoms which require quantum-based treatment are included in a tight-binding calculation, while the remaining ones are included in classical molecular dynamics.

The paper is organized as follows. In Section 2 we briefly comment on the method used to handshake the tight-binding and molecular dynamics methods and describe in short the tight-binding variant used and the simulation procedure. In Section 3 we present the results and a short discussion thereof. Section 4 contains conclusions and final remarks.

2. COMPUTATIONAL METHOD

2.1. Handshaking TB and MD

That a portion of a system has to be extracted for a separate quantum-based computation, performed in isolation from the surrounding atoms, constitutes the main difficulty of cross-scaling computations. Arbitrary cessation of bonds at the TB/MD interface results in a significant disruption of forces in the vicinity of atoms with now unsaturated valencies [7,8]. Link-atom methods traditionally used to counteract this by surrounding the subsystem with virtual atoms rely on bond locality, which prohibits their use for metallic systems.

A gradual shift from forces obtained from tight-binding calculations to the classical forces as the reliability of the former becomes questionable seems to alleviate the aforementioned problem, although at an expense of enlarging the quantum-based region and a lack of strict conservation of energy. In the formalism described in detail in [9] we propose to compute the forces on the atoms in the quantum-based region as a weighted average of forces obtained from tight-binding and classical computations, with the weights in the average changing nonlinearly, favouring the classical forces as the distance from the region's centre (where tight-binding is the most reliable) increases.

2.2. The NRL-TB method

We have decided to use the Naval Research Laboratory total-energy tight-binding (NRL-TB) scheme developed by Mehl and Papaconstantopoulos [10-16] for the quantum-based calculations. This particular variation is of appeal to us because of its good transferability and readily available parametrization for most metals. As the original computer code of Kirchoff *et al*. implementing the method is not freely available, we have implemented it from scratch in our cross-scaling TB+MD program, *nanoTB*, originally developed by M. Białoskórski [17]. For a detailed description, the reader is referred to [9,18].

NRL-TB is a non-orthogonal, two-centre variant of tight-binding, with a dependence of on-site Hamiltonian and overlap matrix elements on generalized local atomic density. This dependence on the environment enables eradication of the repulsive term usually present in the expression for total energy, effectively narrowing the parameter space as justified in [10-12]. In such formulation, the total energy of a system is computed simply as a sum of shifted eigenvalues corresponding to occupied levels. The eigenvalues themselves and the corresponding eigenvectors are obtained by solving the generalized eigenvalue problem.

Electronic forces may then be obtained by means of the Hellmann-Feynman theorem, as described in detail in [19]. The derivatives of the basis set vanish identically in this non-self-consistent formulation of TB [20,21].

2.3. Simulation procedure

Two sets of simulations were carried out: one being cross-scaled TB+MD simulations where atoms in the vicinity of the tool tip were treated with TB, the other being pure MD simulations performed for comparison. The Sutton-Chen many-body potential [22] was employed in all simulations, with a cutoff radius of 12.35 Å, neglecting long-range corrections. The quantum region was cylindrically shaped, with periodic boundary conditions along the *z* direction, while the cylinder axis coincided with the tool tip and moved with the same velocity. The cylinder's diameter was 14 Å: larger than in our previous work [9]. The number of atoms contained within the region varied in time, with a typical value of 300-320 atoms.

The tool was a cuboid of 8x8x7 fcc unit cells, for a total of 2023 atoms, rotated by 45 degrees about the *z* axis and moving along the $[0\bar{1}0]$ direction. Periodic boundary conditions were imposed along the *z* (in-plane) direction, but not along the *x* or *y* directions, implying that the simulated system was that of an infinitely long indenter penetrating an infinitely long, but finitely wide and deep workpiece. Atoms on the bottom surface of the workmaterial were artificially fixed to prevent it from translating upon contact with the tool, while no such fixing was employed for atoms on the sides of the workpiece, in contrast to [1]. For the sake of simplicity, the tool was assumed to be infinitely hard (all forces acting upon it were ignored) and moved not with an application of a constant force but rather with a uniform velocity of 20 m/s, an assumption considerably more realistic than in those of other UPM simulations [1,2].

The simulations were performed at 300K using a Nosé-Hoover thermostat with the temperature coupling time constant of 250 fs [23,24]. Application of more advanced thermostats [25,26] and taking radiative losses into account are envisioned in the near future. A timestep of 2.5 fs was used, and it was shown that energy was conserved to $\Delta E/E = 10^{-6}$ under equilibrium conditions. A fourth-order Gear predictor-corrector was used to integrate the equations of motion.

The simulations started with the tool tip at a distance of 4.75 Å from the workmaterial (cf. Fig. 1), giving the system ample time to equilibrate before contact. The tool was allowed to penetrate 15.25 Å deep into the workpiece during 100 ps, at which point the simulation was terminated.

The effect of workpiece crystal orientation was studied by performing the same simulations with the workpiece carved as a cuboid from a large fcc crystal oriented in (100), (110) and (111) directions, see Table 1.

For the simulation with the workpiece in the (111) crystal orientation, the *z*-dimension mismatch was alleviated by compressing the tool by 2.7% along this direction, to match the workpiece dimension of 24.793 Å.

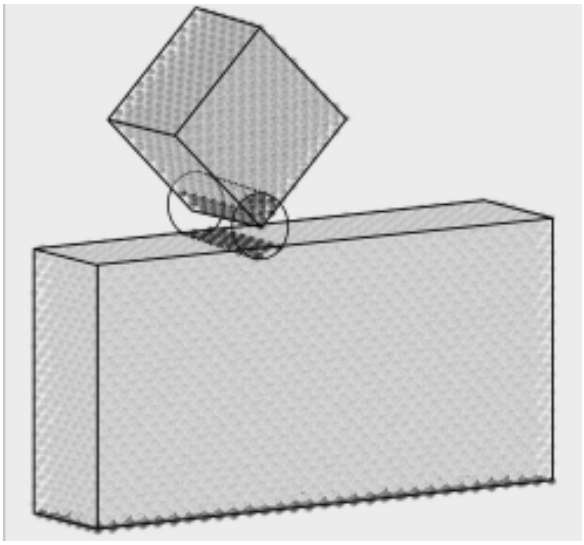

Fig. 1. The initial set-up of a nanoindentation simulation for one of the crystal orientations ((100)) of the workpiece. The edges of the workpiece, the tool and the TB region are outlined. Periodic boundary conditions are in effect along the *z* (in-plane) direction.

3. RESULTS AND DISCUSSION

The normal force experienced by the tool was calculated during the course of all simulations, with the results shown in Fig. 2. Forces were calculated at every timestep and averages over 400 steps (1 ps) are shown. For the simulations involving tight-binding, this force was calculated as the inverse of the force acting on the workmaterial, as direct calculation was impossible because the forces acting on the tool atoms were not computed to reduce

Table 1. Workpiece dimensions and atom count for the three crystal orientations investigated.

(100): 108.750 Å x 54.375 Å x 25.475 Å 13237 atoms.
(110): 107.657 Å x 53.829 Å x 25.475 Å, 12796 atoms.
(111): 108.033 Å x 53.829 Å x 24.793 Å, 12640 atoms.

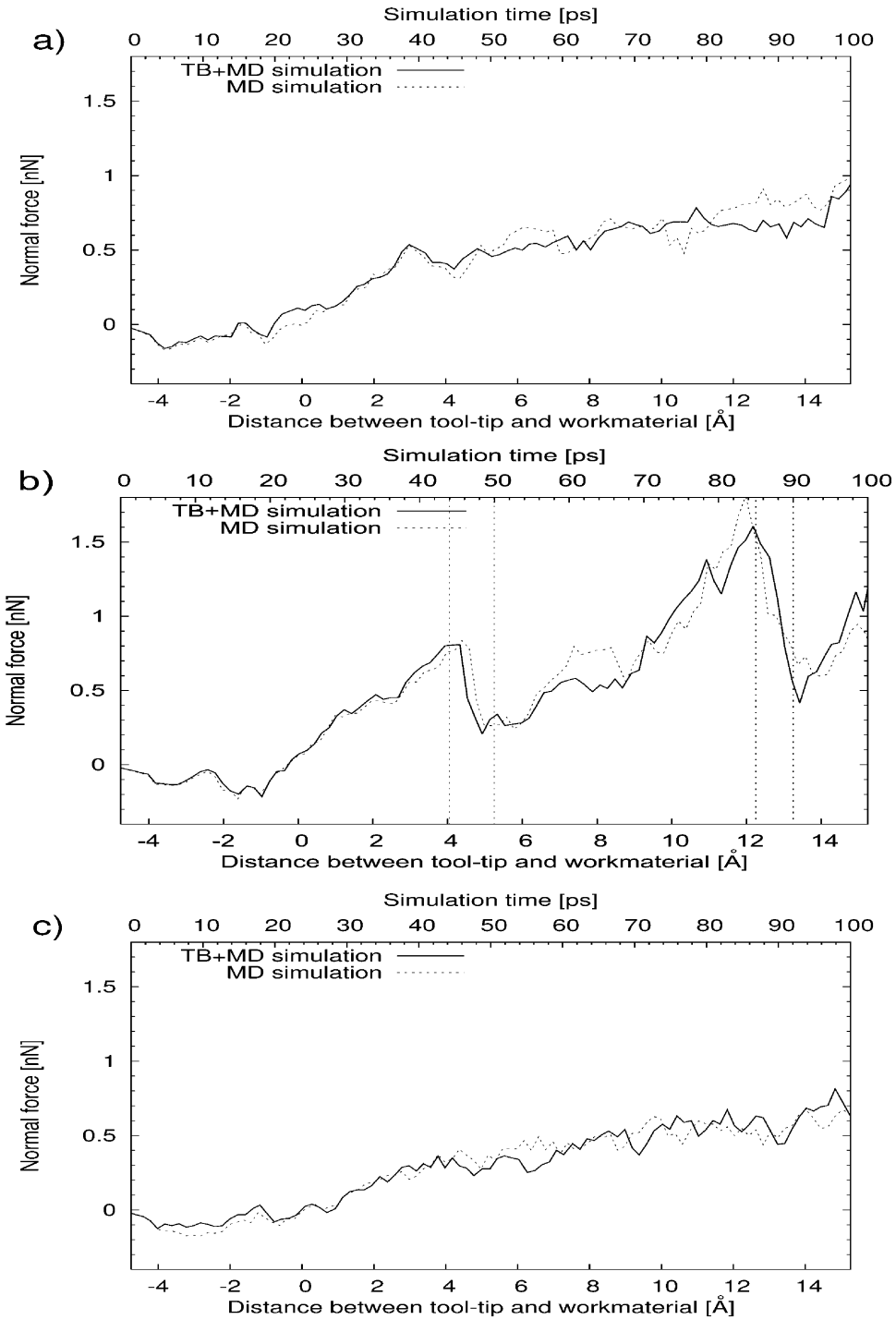

Fig. 2. Comparison of total normal force experienced by the tool with respect to workmaterial orientation ((100), (110), (111), top to bottom) for cross-scaled TB+MD (solid line) and pure MD (dashed line) simulations. Averages collected over 400 steps (1 ps) are shown. The vertical lines in panel b) correspond to the snapshots shown in Fig. 4.

the computational requirements. These are not necessary for the simulation since the tool is infinitely hard.

Consistent with other simulations of UPM [1,2], we have found that the force acting on the tool is initially attractive, but since the tool atoms cannot move in response, it is the workmaterial that begins to wiggle as it is approached by the tool. The magnitude of the force is in the order 0.1-0.2 nN, which is considerably less than reported in [1,2].

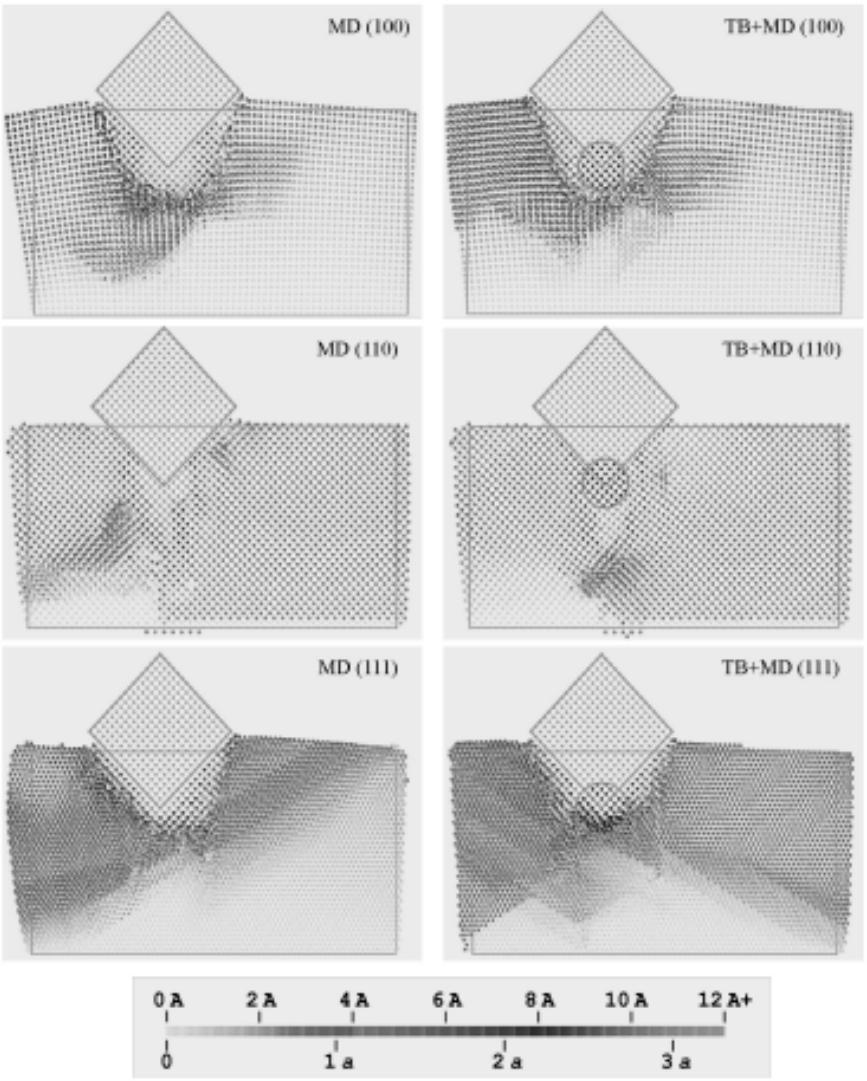

Fig. 3. Snapshots of final configurations obtained after runs of 100 ps, as the tool has penetrated 15.25 Å deep into the workmaterial. The left pane shows results of pure MD simulations, the right pane – the results of cross-scaled TB+MD simulations. The orientations of the workmaterial are (100), (110), (111) (top to bottom). The initial shape of the workmaterial, the TB region and the tool are outlined. The atoms taking part in the TB computation are shown in bright white. Atoms are coloured according to their displacement $|\vec{r}-\vec{r}_0|$ from initial position.

This may be attributed to the fact that the systems compared differ in size, the investigated material (Cu *vs.* Al), the potential used (Sutton-Chen *vs.* Morse), the tool's velocity (20 m/s *vs.* 500 m/s) and the boundary conditions applied. The jump-to-contact phenomenon has been observed, with the top of the workmaterial curving towards the tool at a distance of about 4 Å.

For all three orientations, we have observed that the workpiece gradually yields, deforming plastically as the tool penetrates it, with the force experienced by the tool increasing steadily. Only for the (110) orientation the situation is slightly different. As the tool and the workmaterial have the same crystal orientation and they are not shifted laterally with respect to one another, the tool fits readily into the workmaterial. Thus, apart from the region directly under the tool, the material is less deformed than in the other two orientations (cf. Fig. 3). However, the atoms in the vertical column below the

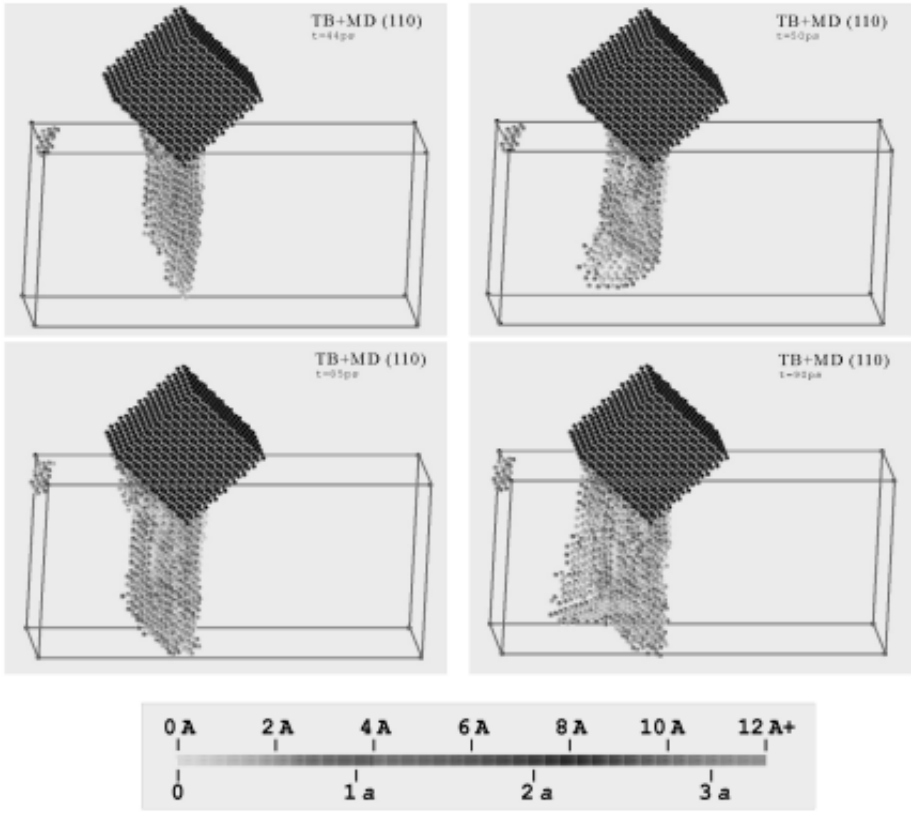

Fig. 4. Configurations of slipped atoms at 44 ps, 50 ps, 85 ps, and 90 ps for the cross-scaled TB+MD simulation, with the workmaterial in the (110) orientation. The initial shape of the workmaterial is outlined for clarity. Only the tool atoms and atoms with a nonzero slip vector are shown.

tool tip, slip into new crystal positions as the tool enters the material. As the tool penetrates deeper, it becomes more difficult to displace the atoms below it, since they lie in energetically favourable positions of an almost perfect crystal. That makes the force gradient experienced by the tool steeper, compared to the other two workmaterial orientations.

The tool movement, however, is unaffected by this repulsive force, and the atoms below it finally need to slip into new positions. As this happens, the force suddenly drops (cf. Fig. 2, panel b). This happens twice during the course of the simulation, at about 45 ps and 85 ps. To illustrate this point, we have determined which atoms have in fact slipped from their original positions, by evaluating the so-called slip vector [27,28] of all the atoms using a computer code from the ANELLI package [29]. Atoms with a nonzero slip vector are assumed to have slipped and are shown in Fig. 4 in snapshots taken just before and just after the atoms have slipped further, resulting in a drop in the force. Apart from a small cluster on the top left of the workmaterial, only the atoms directly below the tool have slipped for this orientation. Moreover, the slipping process leaps forward suddenly at the times shown.

The workmaterial is deformed more easily at the side closer to the tool. We have deliberately placed the tool slightly closer to the left wall of the workmaterial to see if this will influence the indentation process. We find the workmaterial almost unaffected at the right side, which is more distant from the tool tip (cf. Figs. 3 and 5). Although the atoms there move from their initial positions (cf. Fig. 3), this is due to elastic bending of the workmaterial, rather than creation of dislocations, as evidenced by a zero slip vector (cf. Fig. 5). This suggests that the nanoindentation of a much broader piece would probably proceed differently.

We now turn to the differences between the pure MD and the cross-scaled TB+MD simulations. We

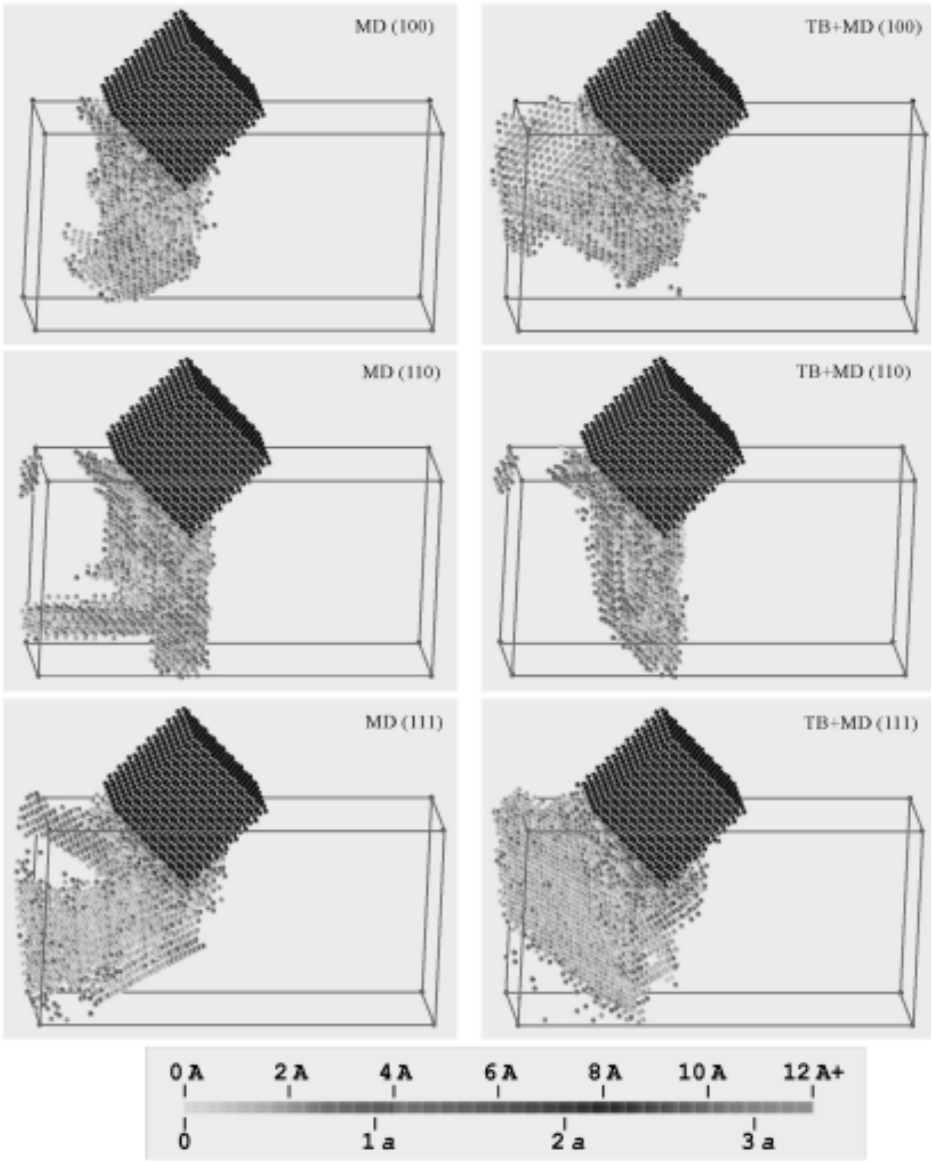

Fig. 5. Snapshots of final configurations obtained after runs of 100 ps, as the tool has penetrated 15.25 Å deep into the workmaterial. The left pane shows results of pure MD simulations, the right pane – the results of cross-scaled TB+MD simulations. The orientations of the workmaterial are (100), (110), (111) (top to bottom). The final positions of the tool atoms are shown and the initial shape of the workmaterial is outlined for clarity. Atoms are coloured according to the magnitude of the slip vector, only atoms with a nonzero slip vector are shown.

did not expect these to be very pronounced because of the small number of atoms that we could treat using the tight-binding method. Since $O(N^3)$ direct diagonalization was used to obtain the energy eigenvalues, the computational cost of the calculation would rise prohibitively with larger region sizes. Furthermore, only the atoms in the inner part of the region are in practice driven by the quantum-based forces due to the nature of the TB/MD interfacing method used [9].

Post factum, it also seems that centering the TB region on the tool tip was not the best choice. A look at Fig. 3 reveals that the atoms within the region are in fact not heavily displaced from equilibrium positions, as they tend to align with the tool surfaces. Placing the region several atomic dis-

tances *below* the tool tip would probably allow quantum calculations to be utilized better. In fact, preliminary calculations with the region placed 5.13 Å (4 atomic layers) below the tool tip have shown more promising results, these will be presented elsewhere.

Nevertheless, we can observe differences in how the simulations proceeded, depending on whether the tight-binding calculation was performed or not. These differences are best seen by comparing the left and right panels of Figs. 3 and 5, and are readily visible for all crystal orientations. For the (100) orientation, we can observe that the left side of the workmaterial shears slightly in the *xy* plane in the TB+MD simulation, while this effect is absent in the pure MD simulation.

Please note how the *xy* displacement of the atoms on the left side in the MD simulation does not depend on the *z* (in-plane) coordinate. This is further evidenced by Fig. 5, where an additional plane of slipped atoms is revealed in this very part of the system, only in the TB+MD simulation.

For the (110) orientation, we note an additional direction of slip develops in the MD simulation, but not in the TB+MD simulation. As the column of slipped atoms nears the bottom of the workmaterial it becomes more difficult for the atoms to slip further, as the bottom layer is fixed in place and the dislocations cannot (in principle) propagate further. Unfortunately, a limitation of the simulation conditions manifests itself here – the force acting on the atoms in the penultimate layer is so large that several atoms manage to squeeze through the fixed layer and find themselves in crystal positions below the workmaterial. The remaining atoms behave differently in the classical and the TB+MD simulations. In the former, an additional horizontal slip plane develops (cf. Fig. 5), easing the atoms in the column under the tool to positions close to those of a perfect crystal. This does not happen in the MD simulation, with the dislocations piling up several layers above the bottom of the workmaterial (best seen in Fig. 3).

Finally, we can observe slight differences in the final configurations for the (111) orientation. The slip planes that originate in both simulations are aligned differently (cf. Fig. 5), resulting in a different redistribution of stress, which in turn causes the workmaterial to shear more in the cross-scaled simulation and bend more in the classical simulation.

4. CONCLUSION

We have carried out cross-scaling, molecular-dynamics simulations of nanoindentation of copper with an infinitely hard tool, with atoms in the vicinity of the tool tip driven by forces obtained from a tight-binding computation. These were performed using a proprietary computer code, *nanoTB*, implementing the NRL-TB total-energy tight-binding method and interfacing it with non-equilibrium molecular dynamics using the method described in [9].

Three crystal orientations of the workmaterial were examined and classical molecular dynamics simulations were performed as a reference. Dislocations were found to propagate differently in the cross-scaled and reference simulations, despite the fact that the quantum-based region was rather small (14 Å in diameter). It is difficult to judge whether the differences in systems' behaviour are attributable to the fact that tight-binding computations were performed for certain atoms, producing markedly different results or are purely incidental.

The force experienced by the tool was calculated and the differences between cross-scaling and reference simulations were found to be insignificant. This may be a consequence of the fact that the force in question is a collective property, depending only on the positions of the atoms in the vicinity of the tool and not on how dislocations propagate in other parts of the system. At the same time, this may as well indicate that the tight-binding region is not large enough or inadequately placed. Similar simulations with a region of 20 Å in diameter are in progress to clarify this important issue.

ACKNOWLEDGEMENTS

The simulations were performed at the TASK Computer Centre in Gdansk, Poland. The work has been sponsored by the Polish Ministry of Science and Information Technology, under grant number 3 T11F 026 29, and the Ministry of Science and Higher Education, under grant number N519 019 31/3498.

REFERENCES

[1] R. Komanduri, N. Chandrasekaran and L. M. Raff // *Wear* **240** (2000) 113.
[2] R. Komanduri, N. Chandrasekaran and L. M. Raff // Wear **242** (2000) 60.

[3] M. Białoskórski, M. Rychcik-Leyk, J. Rybicki and G. Bergmański // *Proc. of the 9-th Workshop of PTSK Koszalin-Osieki* **9** (2002) 13, In Polish.
[4] W. G. Hoover, A. J. De Groot and C. G. Hoover // *Computers in Physics* **6** (1992) 155.
[5] W. G. Hoover, C. G. Hoover, I. F. Stowers, A. J. De Groot and B. Moran, In: *Microscopic Simulations of Complex Flows, a NATO Advanced Science Institute Series* (Plenum, New York, 1990), p. 315.
[6] Wm. G. Hoover and C. G. Hoover // *phys. stat. sol. (b)* **242** (2005) 585.
[7] J. Q. Broughton, F. F. Abraham, N. Bernstein and E. Kaxiras // *Phys. Rev. B* **60** (1999) 2391.
[8] X. P. Long, J. B. Nicholas, M. F. Guest and R. L. Ornstein // *J. Mol. Struct.* **412** (1997) 121.
[9] M. Bobrowski, J. Dziedzic and J. Rybicki // *phys. stat. sol. (b)*, in print.
[10] M. Mehl and D. Papaconstantopoulos, In: *Topics in Computational Materials Science*, *Ch. V*, ed. by C. Y. Fong (World Scientific, Singapore, 1998), p. 169.
[11] D. Papaconstantopoulos and M. Mehl, In: *Proc. of the International Symposium on Novel Materials, Bhubaneswar, India, March 3-7, 1997*, ed. by B.K. Rao, 393 (198).
[12] R. Cohen, M. Mehl and D. Papaconstantopoulos // *Phys. Rev. B* **50** (1994) 14694.
[13] M. Mehl, D. Papaconstantopoulos, N. Kioussis and M. Herbranson // *Phys. Rev. B* **61** (2000) 4894.
[14] F. Kirchoff, M. Mehl, N. Papanicolaou, D. Papaconstantopoulos and F. Khan // *Phys. Rev. B* **63** (2001) 195101.
[15] Y. Mishin, M. Mehl, D. Papaconstantopoulos, A. Voter and J. Kress // *Phys. Rev. B* **63** (2001) 224106.
[16] D. Papaconstantopoulos, M. Lach-hab and M. Mehl // *Physica B* **296** (2001) 129.
[17] M. Białoskórski and J. Rybicki, *Proc. of the 8-th Workshop of PTSK Gdansk-Sobieszewo* **8** (2001) 22 , in Polish.
[18] J. Dziedzic, *nanoTB: User's manual*, http://www.mif.pg.gda.pl/homepages/jaca/grant/manual.
[19] J. Dziedzic // *TASK Quart.* **11** (2007), in print.
[20]. R. Rudd, private correspondence.
[21] M. Kabir, A. Mookerjee and A. K. Bhattacharya // *Phys. Rev. A* **69** (2004) 043203.
[22] A. P. Sutton and J. Chen // *Phil. Mag. Lett.* **61** (1990) 139.
[23] W. G. Hoover // *Phys. Rev. A* **31** (1985) 1695.
[24] S. Nosé // *Mol. Phys.* **52** (1984) 255.
[25] R. G. Winkler // *Phys. Rev. A* **45** (1992) 2250.
[26] A. C. Brańka and K. W. Wojciechowski // *Phys. Rev. E* **63** (2000) 3281.
[27] J. A. Zimmerman, C. L. Kelchner, P. A. Klein, J. C. Hamilton and S. M. Foiles // *Phys. Rev. B* **87** (2001) 165507.
[28] O. Rodriguez de la Fuente, J. A. Zimmerman, M. A. Gonzalez, J. de la Figuera, J. C. Hamilton, W. W. Pai and J. M. Rojo // *Phys. Rev. Lett.* **88** (2002) 36101.
[29] J. Rybicki, G. Bergmański and G. Mancini // *J. Non-Cryst. Solids* **293-295** (2001) 758.